Cosmology with the kinematic Sunyaev-Zeldovich effect: Breaking the optical depth degeneracy with fast radio bursts

Mathew S. Madhavacheril,[1] Nicholas Battaglia,[2,3] Kendrick M. Smith,[4] and Jonathan L. Sievers[5,6]
[1]*Princeton University, Department of Astrophysical Sciences, Princeton, New Jersey 08540, USA*
[2]*Department of Astronomy, Cornell University, Ithaca, New York 14853, USA*
[3]*Center for Computational Astrophysics, Flatiron Institute, 162 5th Avenue, New York, New York 10010, USA*
[4]*Perimeter Institute for Theoretical Physics, Waterloo, Ontario N2L 2Y5, Canada*
[5]*Department of Physics, McGill University, 3600 Rue University, Montreal, Quebec H3A 2T8, Canada*
[6]*School of Chemistry and Physics, University of KwaZulu-Natal, Westville Campus, Durban 3209, South Africa*

(Received 28 March 2019; published 25 November 2019)

The small-scale cosmic microwave background is dominated by anisotropies from the kinematic Sunyaev-Zeldovich (kSZ) effect, and upcoming experiments will measure it very precisely, but the optical depth degeneracy limits the cosmological information that can be extracted. At the same time, fast radio bursts (FRBs) are an exciting new frontier for astrophysics, but their usefulness as cosmological probes is currently unclear. We show that FRBs are uniquely suited for breaking the kSZ optical depth degeneracy. This opens up new possibilities for constraining cosmology with the kSZ effect, and new cosmological applications for FRBs.

DOI: 10.1103/PhysRevD.100.103532

I. INTRODUCTION

As photons from the cosmic microwave background (CMB) travel through the Universe, a small fraction interact with free electrons. The kinematic Sunyaev-Zeldovich (kSZ) effect [1] is the result of CMB photons Compton scattering off free electrons that have nonzero peculiar velocities with respect to the CMB rest frame, which lead to additional anisotropies in the observed CMB radiation. As a result, we observe a small shift in the CMB temperature in the direction of those free electrons. This shift is proportional to the integrated momentum along the line of sight. Thus, kSZ measurements are potentially powerful observational probes of the peculiar velocities of systems of ionized gas that trace the total distribution of matter (e.g., [2–5]). Since the small-scale CMB is dominated by kSZ fluctuations and upcoming CMB surveys will measure it very precisely [6,7], mapping the peculiar velocity distribution of the Universe with kSZ will provide competitive constraints on primordial non-Gaussianity [8]. Velocities probe the cosmological growth rate, which can allow further constraints on modified gravity models, the dark energy equation of state, and the sum of neutrino masses (e.g., [5,6,8–14]).

The cosmological growth rate measured through the kSZ effect is however perfectly degenerate with the optical depth of galaxies or clusters (e.g., [15,16]), leading to an overall uncertainty in the inferred amplitude of the growth rate. This degeneracy with the optical depth is the limiting systematic uncertainty for measurements of the cosmological growth rate from kSZ tomography (e.g., [7,9,13]).

Recent detections of multiple fast radio burst sources (FRBs[1]) along with theoretical models strongly suggest that there exist transient radio events originating (possibly) from energetic events at cosmological redshifts that are detectable with a rate greater than one per day (e.g., [17–19]). With future upgrades and outrigger stations, instruments like HIRAX [20] should localize of order 10 FRBs per day with subarcsecond accuracy that will enable one to acquire redshifts [21]. Plasma along the line of sight delays the FRBs in a frequency-dependent manner, with the delay in seconds approximately equal to $4.15 \times 10^{-3}\ \mathrm{DM}/\nu^2_{\mathrm{GHz}}$ where DM is the *dispersion measure*, in $\mathrm{pc}/\mathrm{cm}^3$, and is equivalent to the optical depth τ due to Compton scattering: $\mathrm{DM} = (4.87 \times 10^5\ \mathrm{pc\,cm^{-3}})\tau$. Radio telescopes measure the DMs associated with these events quite precisely (typical measurement accuracies are 0.1%), which receive contributions from the host galaxy, the Milky Way, and any intervening free electrons (e.g., [22]). The third of these contributions is of great interest to the extragalactic and cosmological communities. With the promise of thousands of FRBs in the future, theoretical ideas and forecasts have been published regarding measuring the baryon content in the intergalactic medium (e.g., [23]) and the circumgalactic medium (e.g., [24]), regarding constraining the reionization

[1]Hereafter, FRBs refer to the sources, not the bursts.

epoch [25], and regarding measuring three-dimensional clustering of free electrons [26] to name a few.

In this work, we propose to directly measure the galaxy optical depth through the contribution to FRB DMs from scattering off of intervening free electrons, using the cross-correlation between the galaxy sample used in the kSZ measurement and a map of FRB dispersion measures. This cross-correlation can be directly interpreted as the galaxy optical depth as it is measuring the galaxy-electron power spectrum $P_{\rm ge}(k)$, thus breaking the optical depth degeneracy and allowing for subpercent constraints on the growth rate. We focus on the information on the cosmological growth rate that we can extract with thousands or more of localized FRB measurements in combination with kSZ measurements made by upcoming CMB and galaxy surveys. We note that a recent paper [27] investigated the possibility of using FRBs for cosmological tests, but found no interesting applications other than constraining the ionized gas distribution. We show in this work that constraining ionized gas (specifically, the galaxy-electron correlation) with FRBs enables cosmological applications of the kSZ effect.

II. THE GALAXY-ELECTRON SPECTRUM MEASURED WITH FRBs

The DM along a line of sight should be correlated with the density of foreground galaxies in that direction, since some of the electron fluctuations contributing to the DM originate from those galaxies. We are thus interested in cross-correlating foreground galaxies with a map of DMs (not spatial locations) from FRBs. Note that this does not require FRBs to be clustered or for them to have redshift overlap with the galaxies. They instead act as a backlight for the free electrons in these galaxies, like quasars act for neutral hydrogen. The FRBs need to be localized with redshift information sufficient to inform whether or not the FRB in any given FRB-galaxy pair is behind the galaxy.

Because the DM is an integrated quantity along the line of sight, it is convenient to do the forecast using two-dimensional fields (not three dimensional). For this preliminary investigation into the feasibility of using FRBs for cosmology, we work with a simplified geometry. We consider a thin shell of foreground galaxies, specifically a sample with a mean redshift of 0.75, redshift shell width of 0.3, and number density of $\sim 1.7 \times 10^{-4}$ Mpc^{-3} expected to be provided by surveys like the Dark Energy Spectroscopic Instrument (DESI) [28]. All the FRBs are assumed to lie in a thin background shell centered at $z = 1$. In this thin-shell geometry, we can treat all fields in sight as two-dimensional fields.

Let $(\chi_g - \Delta\chi_g/2, \chi_g + \Delta\chi_g/2)$ be the comoving distance interval spanned by the foreground galaxies, and let $(\chi_f - \Delta\chi_f/2, \chi_f + \Delta\chi_f/2)$ be the comoving distance interval spanned by the background FRBs. We use the notation $(\cdot)_g$ to mean evaluated at the redshift of the galaxies; e.g., z_g is the galaxy redshift.

We assume that the separation between the foreground and background shells is large enough that there are no spatial correlations between foreground galaxies and the spatial locations (or the host DMs) of background FRBs. Thus any galaxy-DM correlations can be attributed to correlations between the galaxies and the electrons along the line of sight in those galaxies.

The line-of-sight integral for the dispersion measure is (see, e.g., [29])

$$D(\hat{\mathbf{n}}) = n_{e0} \int_0^{\chi_f} d\chi (1+z)(1+\delta_e(\hat{\mathbf{n}}, z)), \tag{1}$$

where $\hat{\mathbf{n}}$ is the line-of-sight direction, n_{e0} is the mean number density of free electrons at $z = 0$, and χ is the comoving distance. In the Limber approximation (equivalent to a small-angle approximation that is valid for the scales we consider), the cross-correlation between the two-dimensional DM field, D, and the two-dimensional galaxy overdensity field, δ_g, is

$$C_l^{Dg} = n_{e0} \frac{1+z_g}{\chi_g^2} P_{\rm ge}(k, z_g)_{k=l/\chi_g}, \tag{2}$$

where the C_l notation denotes angular power spectra at angular wave number or multipole l, and $P_{\rm ge}$ is the three-dimensional galaxy-electron cross power spectrum as a function of the magnitude k of the three-dimensional Fourier wave number $\mathbf{k}$. Our proposed observable C_l^{Dg} thus measures the power spectrum $P_{\rm ge}$, which is an important quantity that captures how the free electron overdensity δ_e is correlated with the galaxy overdensity δ_g. As explained in [7], the very same power spectrum $P_{\rm ge}$ is also measured by kSZ tomography. However, for cosmological applications of kSZ, $P_{\rm ge}$ appears in a nuisance parameter that multiplies the cosmologically informative cross power spectrum of galaxies and the cosmic velocity field P_{gv} (e.g., [7]). This motivates our external measurement of $P_{\rm ge}$ from FRB DMs.

To complete our forecast for the signal-to-noise ratio (SNR) of C_l^{Dg}, we also need the associated autopower spectra (again making the Limber approximation),

$$C_l^{DD} = n_{e0}^2 \int_0^{\chi_f} d\chi \frac{(1+z)^2}{\chi^2} P_{ee}(k, z)_{k=l/\chi}, \tag{3}$$

$$C_l^{gg} = \frac{1}{\chi_g^2(\Delta\chi_g)} P_{gg}(k, z_g)_{k=l/\chi_g}, \tag{4}$$

where P_{ee} and P_{gg} are the electron and galaxy autopower spectra, respectively.

The small-scale power spectra above are calculated in the halo model following [7], with contributions from

clustering of electrons and galaxies (the two-halo term) and from the shape of the profiles of the electron and galaxy distributions (the one-halo term). The calculated two-dimensional power spectra are shown in Fig. 1. When we "observe" the two-dimensional DM field, D, with a discretely sampled catalog of FRBs, there is an associated noise power spectrum N_l^{DD} given by

$$N_l^{DD} = \frac{\sigma_D^2}{n_f^{2d}}. \tag{5}$$

Here, n_f^{2d} is the number density (per steradian) of FRBs, and σ_D^2 is the total variance of the DMs. The latter is the sum of three contributions: intrinsic scatter in the FRB host's DM, residual uncertainty in the DM of our Galaxy, and a term $\int d^2l/(2\pi)^2 C_l^{DD}$ from electron fluctuations along the line of sight that is not associated with galaxies we are cross-correlating with, the cosmological variance. We do not worry about keeping track of these contributions separately, since the host contribution is a free parameter anyway. Since the RMS scatter of the DMs σ_D is currently uncertain, we show forecasts for various plausible values given current detections of FRBs. We chose the range to be from 100 to 1000 pc/cm^3. This range is motivated by empirical measurements of the intrinsic DM of the host of the repeating FRB [30], which has DM of $\lesssim$324 pc/cm^3 [21]. The cosmological DM RMS scatter is of order 100–1000 pc/cm^3 from our halo model calculations and from simulations [22]. The DM of our Galaxy varies dramatically depending on sky location; however, models exist (e.g., [31]) to remove this contribution with only a small, uncorrelated residual left to contribute to the variance.

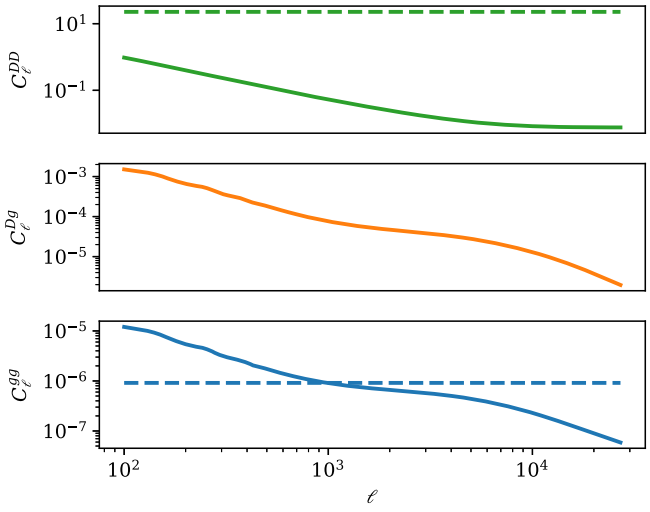

FIG. 1. Power spectra of the FRB dispersion measure and galaxy density fields calculated under the thin-shell approximation. The solid green, orange, and blue lines show the FRB DM autopower spectrum (in $(\frac{\text{pc}}{\text{cm}^3})^2$), the galaxy-DM cross power spectrum (in $\frac{\text{pc}}{\text{cm}^3}$), and the galaxy autopower spectrum (dimensionless), respectively. The blue dashed line shows the shot noise per mode in the DESI galaxy survey. The green dashed line shows the effective noise per mode in the FRB DM field for a DM RMS scatter of 300 $\frac{\text{pc}}{\text{cm}^3}$ and total number of FRBs of 10 000.

In terms of the above definitions, the total S/N of the DM-galaxy cross power is given by

$$\text{S/N}^2 = \Omega \int \frac{d^2l}{(2\pi)^2} \frac{(C_l^{Dg})^2}{(\mathcal{N}_l^{Dg})^2}, \tag{6}$$

where

$$(\mathcal{N}_l^{Dg})^2 = (C_l^{gg} + 1/n_g^{2d})(C_l^{DD} + \sigma_D^2/n_f^{2d}), \tag{7}$$

n_g^{2d} is the number density of galaxies in the galaxy survey (per steradian), and Ω is the angular size of the survey in steradians that accounts for the partial sky coverage fraction f_{sky} of the survey overlap through $\Omega = 4\pi f_{\text{sky}}$.

Using Eqs. (2) and (6), we can also obtain the uncertainty on the band powers of the galaxy-electron power inferred from the DM-galaxy cross-correlation (see Appendix A for details),

$$\Delta P_{\text{ge}} = \frac{\chi_g}{n_{e0}(1+z_g)} \left(\Omega \int_{k_{\text{min}}}^{k_{\text{max}}} \frac{kdk}{2\pi} \frac{1}{(\mathcal{N}_l^{Dg})^2} \right)^{-1/2}_{l=k\chi_g}. \tag{8}$$

In Fig. 2, we show the galaxy-electron power spectrum along with the uncertainties on its band powers from a measurement made using the DESI galaxy sample cross-correlated with 10^4 FRB DMs, assuming the simplified geometry described above and a DM RMS scatter of 300 $\frac{\text{pc}}{\text{cm}^3}$. For comparison, we also show the uncertainties on the P_{ge} from a kSZ tomography [7] measurement using the proposed CMB-S4 experiment [32] and DESI, where we have assumed that the factor that multiplies P_{ge} and depends on the cosmologically informative power spectrum P_{gv} has been fixed to a fiducial cosmology. We see that FRB DMs measure P_{ge} over a broad range of scales, while as noted in [7], kSZ tomography measures it very well only in a small range of scales in the one-halo regime.

III. THE COSMOLOGICAL CONNECTION

The FRB-determined measurement of the small-scale cross-power spectrum of galaxies and electrons $P_{\text{ge}}(k)$ detailed in the previous section can be used to break a degeneracy that limits the cosmological utility of kSZ tomography. Since the kSZ effect arises from the Doppler shifting of CMB photons that Compton scatter off free electrons with bulk radial velocities, the large-scale cosmic velocity field modulates the cross-power spectrum of the CMB temperature and galaxy overdensity field. This idea allows one to infer the large-scale cosmic velocity field

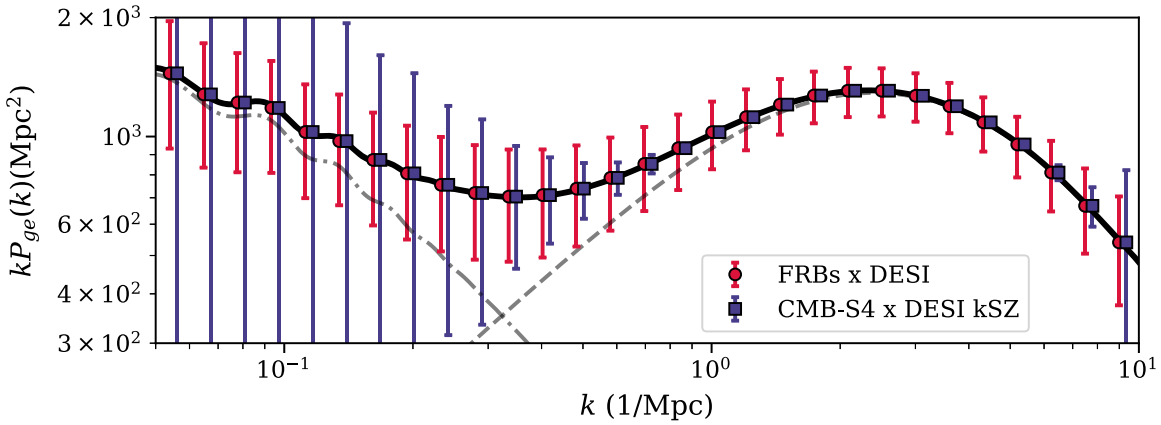

FIG. 2. The cross-power spectrum of galaxies and electrons as measured either through kSZ tomography with CMB-S4 and DESI (blue) with fixed cosmology, or through cross-correlation of dispersion measures of 10^4 FRBs with DESI galaxies (red), where the RMS scatter of DMs is assumed to be 300 $\frac{\mathrm{pc}}{\mathrm{cm}^3}$. FRB DMs measure the power over a broad range of scales including the two-halo regime (dot-dashed), while kSZ tomography provides an extremely tight measurement in the one-halo dominated regime (dashed). Our lack of knowledge of the galaxy-electron power spectrum on these small scales limits our ability to use large-scale velocities from kSZ for cosmology. This degeneracy can be broken using the externally measured FRB cross-correlation.

from a combination of the CMB temperature anisotropies as measured by a CMB survey and the positions of galaxies as measured by a galaxy survey [7,33] on small scales. However, this velocity field can only be inferred up to an overall constant b_v since the kSZ effect is proportional to both the bulk radial velocity and the overdensity of free electrons. This unknown constant b_v is in fact an integral over precisely the small-scale galaxy-electron power spectrum $P_{\mathrm{ge}}(k)$ that can be measured with FRB DMs.

On large scales where linear theory is valid, the velocity reconstruction from kSZ tomography is directly proportional to the cosmic growth rate $f(a) \approx \frac{d \ln D(a)}{d \ln a}$, where $D(a)$ is the growth factor for the matter spectrum that evolves as $P_{mm}(a) = D^2(a) P_{mm}(a = 1)$ and a is the expansion scale factor. Since the velocity reconstruction is uncertain up to the amplitude b_v, in order to convert a kSZ tomography measurement to cosmological information on massive neutrinos, dark energy perturbations, modified gravity, and other physics that can affect the growth rate, one needs an external measurement of b_v, or equivalently of $P_{\mathrm{ge}}(k)$. This is the so-called "optical depth degeneracy."[2] To summarize, the program of constraining cosmology using linear theory with large-scale ($k \ll 0.1$ Mpc^{-1}) velocities from kSZ requires knowledge of an integral of the galaxy-electron power spectrum over extremely nonlinear small scales (0.1 Mpc$^{-1} < k < 10$ Mpc^{-1}).[3]

We have seen in the previous section that FRB DMs can provide this external measurement of small-scale $P_{\mathrm{ge}}(k)$. At the back-of-the-envelope level, a 1% constraint on $P_{\mathrm{ge}}(k)$ from FRBs (or equivalently S/N $= 100\sigma$ on C_ℓ^{Dg}) could translate to a 1% constraint on the velocity bias b_v. However, in practice, the velocity bias information in the FRB measurement is somewhat lower, because FRB DMs measure $P_{\mathrm{ge}}(k)$ over a broad range of scales while (due to the squeezed bispectrum origin of the kSZ effect) the optical depth degeneracy is sourced primarily by small scales in the one-halo regime. In Appendix B, we obtain the one-sigma constraint $\sigma(b_v)$ from FRB DMs properly accounting for this.

In Fig. 3 we show both the raw SNR for the measurement of C_ℓ^{Dg} [or $P_{\mathrm{ge}}(k)$] using FRB DMs and the DESI galaxy survey [from Eq. (6)], and the closely related relative uncertainty on the velocity bias calculated using Eq. (B6). As expected the SNR on the velocity bias is slightly lower. The SNR saturates at high FRB number density when it becomes limited by the sample variance C_l^{DD} in the contribution to DMs from intervening free electrons.

We can now obtain constraints on the cosmic growth rate that incorporate prior information on b_v from FRBs. The large-scale velocity field in linear theory inferred from kSZ tomography is now

$$\hat{v}_{\mathrm{rec}}(\mathbf{k}) = b_v \mu \frac{faH}{k} \delta_m(\mathbf{k}), \tag{9}$$

where $\mathbf{k}$ is the three-dimensional wave vector, $\mu = k_r/k$, for the radial component of the wave vector k_r (along the line of sight), H is the Hubble constant at the redshift of the galaxy sample, and δ_m is the matter overdensity. The velocity reconstruction is performed over small-wavelength modes k_S in the high-resolution CMB survey and the galaxy survey. The modes k_S are limited to 0.1 Mpc$^{-1} < k < 10$ Mpc^{-1}.

[2]Hereafter, we refer to the unknown quantity (whose priors we obtain from FRBs) as the velocity bias, which can be loosely interchanged with optical depth.

[3]Note however that scale-dependent effects, e.g., scale-dependent galaxy bias from primordial non-Gaussianity, can be constrained extremely well [34].

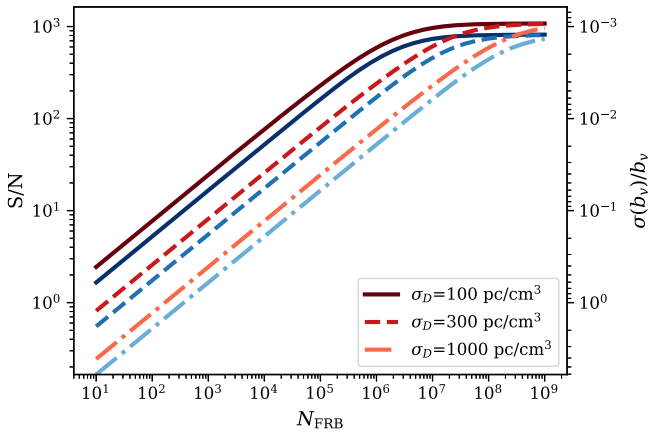

FIG. 3. The signal-to-noise ratio (S/N) of the cross-correlation of DMs from FRBs with the DESI galaxy survey (red, left vertical axis) and the closely related relative uncertainty on the velocity bias or equivalently the galaxy optical depth (blue, right vertical axis), as a function of the number of FRBs, $N_{\rm FRB}$, in the background of DESI galaxies (over an overlap $f_{\rm sky} = 0.2$). The S/N depends strongly on the currently poorly constrained RMS scatter of intrinsic DM of the FRB host galaxy, here shown for various plausible values. Sample variance in the free electron fluctuations causes the S/N to saturate to $\approx 10^3$.

We marginalize over b_v for a fiducial value of $b_v = 1$ but with the Gaussian prior determined earlier that depends on the number of FRBs, $N_{\rm FRB}$.

We consider survey combinations comprising DESI and CMB-S4 and leave $N_{\rm FRB}$, which are localized with redshifts as a free parameter. The assumed configurations of DESI and CMB-S4 can be found in [7]. DESI and CMB-S4 are used to obtain the above velocity reconstruction. The reconstruction $\hat{v}_{\rm rec}$ can then be combined with the galaxy overdensity field δ_g from DESI. The noise on the velocity reconstruction is given by [7]

$$N_{vv}(k) = \mu^{-2}\frac{\chi_g^2}{K_g^2}\left[\int \frac{k_S dk_S}{2\pi}\left(\frac{P_{\rm ge}(k_S)^2}{P_{gg}^{\rm tot}(k_S)C_l^{\rm TT,tot}}\right)_{l=k_S\chi_g}\right]^{-1}, \tag{10}$$

where K_g is the kSZ radial weight function (defined in [7]) at the galaxy shell redshift, χ_g is the comoving distance to the galaxy shell redshift, and $C_l^{\rm TT,tot}$ is the total angular power spectrum of CMB temperature anisotropies, including the late-time and reionization kSZ and foreground residuals after multifrequency cleaning.

This combination gives us the following power spectra,

$$P_{gg}(k,\mu) = (b_g + f(z)\mu^2)^2 P_{mm}(k), \tag{11}$$

$$P_{gv}(k,\mu) = b_v\left(\frac{f(z)aH(z)}{k}\right)(b_g + f(z)\mu^2)P_{mm}(k), \tag{12}$$

$$P_{vv}(k,\mu) = b_v^2\left(\frac{f(z)aH(z)}{k}\right)^2 P_{mm}(k), \tag{13}$$

where b_g is the linear galaxy bias, P_{gv} is the galaxy-velocity cross power spectrum, P_{gg} is the galaxy autopower spectrum, and P_{vv} is the velocity autopower spectrum. We only include the RSD term $f\mu^2$ [35] in Eqs. (11) and (12) if explicitly mentioned from here on. As mentioned in [7], the velocity reconstruction formalism explicitly shows how the octopolar pair sum estimator of [36] that utilizes higher moments of the galaxy-velocity correlation in redshift space can break the optical depth degeneracy. However, DMs from FRBs can be used as an independent way of breaking the optical depth degeneracy that is not affected by potential systematics in RSD measurements [37]. We thus do not include the $f\mu^2$ term in our baseline forecasts.

We can now forecast for cosmological parameters by constructing the Fisher matrix for the modes of the galaxy overdensity field and the reconstructed velocities

$$F_{ab} = \frac{V}{2}\int \frac{2\pi dk k^2}{(2\pi)^3}\int_{-1}^{1} d\mu {\rm Tr}[C_{,a}C^{-1}C_{,b}C^{-1}] \tag{14}$$

with covariance matrix

$$C = \begin{bmatrix} P_{gg} + N_{gg} & P_{gv} \\ P_{gv} & P_{vv} + N_{vv} \end{bmatrix}, \tag{15}$$

where V is the total volume of the overlapping survey in Mpc^3, and $N_{gg} = 1/n_{\rm gal}$ is the shot noise contribution to the large-scale galaxy power spectrum, with $n_{\rm gal} = 1.7 \times 10^{-4}$ Mpc^{-3} assumed for DESI. We consider a cosmological model parametrized by the scale-independent growth rate f at $z = 0$ and the amplitude of matter fluctuations σ_8 at $z = 0$. We perform a Fisher analysis for the parametrization $\{b_g\sigma_8, f\sigma_8, b_v\}$ around fiducial parameters $\{b_g = 1.51, f = 0.53, \sigma_8 = 0.83, b_v = 1\}$ and use priors on b_v obtained using the results in Appendix B. We then obtain the marginalized constraint on $f\sigma_8$ shown in Fig. 4.

IV. RESULTS AND DISCUSSION

We have shown that when the dispersion measures of FRBs are cross-correlated with a galaxy survey, we can reconstruct the galaxy-electron power spectrum $P_{\rm ge}$, which is precisely the observable that breaks the kSZ optical depth degeneracy, thus enabling cosmological applications of the kSZ effect. We find that the cross-correlation of DMs from FRBs with a galaxy survey like DESI is detectable, if around 100–1000 FRBs can be localized with sufficient redshift information to place them behind the DESI sample (Fig. 3). Such measurements translate into constraints on the optical depth of DESI galaxies at the 1%

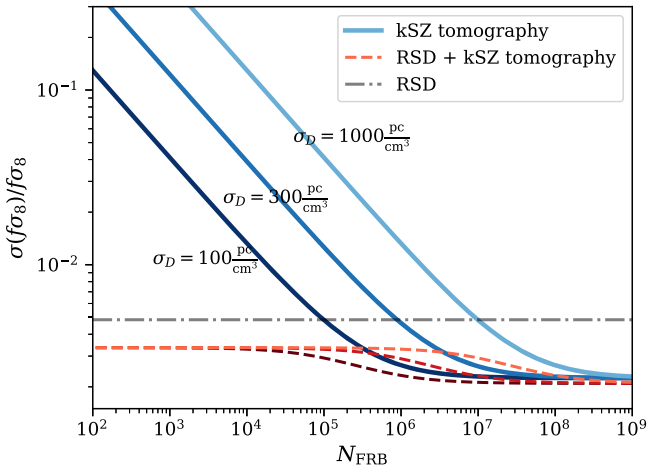

FIG. 4. The uncertainty on the combination of cosmic growth rate and amplitude of matter fluctuations $f\sigma_8$ from kSZ tomography with CMB-S4 and DESI as a function of the number of FRBs, N_{FRB}, available to break the cluster optical depth degeneracy through cross-correlation of FRB DMs with the same DESI galaxy sample. The blue lines show the constraint from kSZ tomography with various shades corresponding to choices of the uncertain RMS scatter of FRB DMs σ_D. If redshift-space distortion (RSD) information is used in conjunction with kSZ (red dashed lines), the degeneracy is already broken to some degree but further improvement is possible with FRBs. The grey dot-dashed line shows the constraint from DESI RSD alone.

level for 100 000 localized FRBs if $\sigma_D = 300$ pc/cm^3. In Fig. 4, we show how such optical depth priors from FRB-galaxy cross-correlations translate to cosmological growth rate measurements from kSZ tomography with CMB-S4 and DESI. We show that <1%-level constraints can be obtained with $N_{\mathrm{FRB}} > 10^5$ and $\sigma_D \sim 300$ pc/cm^3 independent of RSD measurements. Additionally, we show improvements of up to 50% can also be made when combined with RSD for very large N_{FRB} values. These constraints saturate above ∼0.1% due to sample variance in the distribution of electron fluctuations.

The numbers of FRBs considered here are significantly larger than the total number of detected FRBs to date, and no nonrepeating FRBs have been localized to a host galaxy. However, this dearth of observational data is set to change. The MeerKAT key project TRAPUM [38] should localize ∼20 FRBs/year in its coherent mode. The deep synoptic array [24] should be able to localize ∼100 per year in its 200-dish phase. CHIME has already reported new FRBs and could find up to thousands per year. While CHIME currently does not have localization capability, it could, in principle, be added. HIRAX expects to find 10–20 per day, with localization at the ∼30 mas level from southern African outriggers for a large fraction of those. Further in the future, SKA-MID should localize FRBs at 200 times the Parkes rate [39], for $\sim 10^4$ per year. So getting to 10^5 localized FRBs is feasible on a decade timescale with currently planned instruments. Since the FRB detection rate should scale like $A_{\mathrm{eff}}^{1.5}$ for arrays with fixed primary beam, a factor of a few increase in size on experiments like CHIME/HIRAX/DSA could feasibly push this up to $\sim 10^6$ events.

Beyond breaking the optical depth degeneracy, the cross-correlation of DMs from FRBs with galaxy surveys provides constraints on the baryon distribution in galaxies and clusters. On small scales, the shape of $P_{\mathrm{ge}}(k)$ is a measurement of the one-halo electron free electron profile. As previous theoretical works have shown for real space (not Fourier space) (e.g., [23,24,40,41]), this provides valuable information on baryon density profiles of galaxies, groups, and clusters. Additionally, the profiles inferred from FRB DMs are unbiased. Obtaining such profiles provides information on the impact of baryons on the matter power spectrum (e.g., [42]), which is currently unconstrained by empirical measurements, but is extremely important for future cosmological measurements that aim to probe the matter power spectrum on small scales (e.g., [43–45]).

We have chosen the growth rate $f\sigma_8$ in these forecasts as it is a model-independent parametrization for the physics probed by cosmic velocities. The growth rate, however, can be affected by massive neutrinos, dark energy perturbations, and modifications of general relativity. We thus expect that the breaking of the optical depth degeneracy achieved using FRBs put forward in this work can yield significant constraints on extensions of the standard model of cosmology. This also requires going beyond the simplistic cosmological parametrization that we have considered here (for example, incorporating marginalization over the Hubble constant and matter density, while imposing priors from primary CMB measurements). These explorations are left for future work.

ACKNOWLEDGMENTS

We thank Jim Cordes, Colin Hill, and Anze Slosar for comments on an early draft. We are grateful to Matt Johnson and Moritz Münchmeyer who helped develop the halo model code used in this work. We also thank Ue-Li Pen and Vikram Ravi for useful discussions. M. S. M. is grateful to the Perimeter Institute for supporting his visit during which this work was carried out.

APPENDIX A: STATISTICAL ERROR ON P_{ge} BAND POWERS

The statistical error on a C_l^{Dg} band power, defined by an l-range $[l_{\mathrm{min}}, \mathrm{lmax}]$, can be derived as follows. Working in the thin-shell approximation for simplicity, we take Eq. (6) for the total SNR, and restrict the l-integral to obtain the binned SNR,

$$\mathrm{SNR}^2_{\mathrm{bin}} = \Omega \int_{l_{\mathrm{min}}}^{l_{\mathrm{max}}} \frac{ldl}{2\pi} \frac{(C_l^{Dg})^2}{(\mathcal{N}_l^{Dg})^2}. \tag{A1}$$

The statistical error on the band power is then given by

$$\Delta C_l^{Dg} = \frac{C_l^{Dg}}{\mathrm{SNR}_{\mathrm{bin}}} = \left(\Omega \int_{l_{\mathrm{min}}}^{l_{\mathrm{max}}} \frac{ldl}{2\pi} \frac{1}{(\mathcal{N}_l^{Dg})^2}\right)^{-1/2}. \tag{A2}$$

In the thin-shell approximation, C_l^{Dg} is related to $P_{\mathrm{ge}}(k)$ by Eq. (2). Therefore, we can recast the preceding result as the statistical error on a P_{ge} band power over k-range $[k_{\mathrm{min}}, k_{\mathrm{max}}]$ to obtain Eq. (8).

APPENDIX B: VELOCITY BIAS PRIOR

At back-of-the-envelope level, the constraint on b_v is $\sigma(b_v) = 1/\mathrm{SNR}$, where the SNR of the FRB-galaxy cross-correlation was given in Eq. (6). However, this estimate is optimistic, since the SNR is obtained by summing all k-bins, whereas the kSZ velocity bias only depends on P_{ge} in a specific k-range.

To derive a better estimate for $\sigma(b_v)$, which we use in the rest of this work, we recall that the kSZ velocity-bias b_v is defined by

$$b_v = \frac{\int dk_S F(k_S) P_{\mathrm{ge}}^{\mathrm{true}}(k_S)}{\int dk_S F(k_S) P_{\mathrm{ge}}^{\mathrm{fid}}(k_S)}, \tag{B1}$$

where

$$F(k_S) = k_S \frac{P_{\mathrm{ge}}^{\mathrm{fid}}(k_S)}{P_{gg}^{\mathrm{tot}}(k_S)} \left(\frac{1}{C_l^{\mathrm{TT,tot}}}\right)_{l=k_S\chi_g} \tag{B2}$$

and the integration range is over small-scale wave numbers $0.1\ \mathrm{Mpc}^{-1} < k < 10\ \mathrm{Mpc}^{-1}$. We can obtain an estimate for the uncertainty $\sigma(b_v)$ on b_v by relating it to the uncertainty ΔP_{ge} on the band powers of P_{ge} through a quadrature sum of uncertainties, as is appropriate for uncorrelated bins that are normally distributed. To do this, we define a large number of k_S-bins, with width Δk_S. Replacing the integral in the numerator of Eq. (B1) by a sum, the statistical error on b_v is

$$\sigma(b_v)^2 = \frac{\sum F(k_S)^2 (\Delta P_{\mathrm{ge}}(k_S))^2 (\Delta k_S)^2}{(\int dk_S F(k_S) P_{\mathrm{ge}}^{\mathrm{fid}}(k_S))^2}, \tag{B3}$$

where the sum in the numerator runs over k_S-bins. For notational compactness, we rewrite Eq. (8) in the form

$$(\Delta P_{\mathrm{ge}}(k_S))^{-2} = G(k_S)(\Delta k_S), \tag{B4}$$

where we have defined

$$G(k_S) = \left(\frac{\chi_g}{n_{e0}(1+z_g)}\right)^{-2} \left(\frac{k_S\Omega}{2\pi}\right) \times \left(\frac{1}{(C_l^{gg} + 1/n_g^{2d})(C_l^{DD} + \sigma_D^2/n_f^{2d})}\right)_{l=k_S\chi_g}. \tag{B5}$$

Plugging Eq. (B4) into Eq. (B3), we get our final expression for $\sigma(b_v)$,

$$\sigma(b_v)^2 = \frac{\sum F(k_S)^2 G(k_S)^{-1} (\Delta k_S)}{(\int dk_S F(k_S) P_{\mathrm{ge}}^{\mathrm{fid}}(k_S))^2} = \frac{\int dk_S F(k_S)^2 G(k_S)^{-1}}{(\int dk_S F(k_S) P_{\mathrm{ge}}^{\mathrm{fid}}(k_S))^2}, \tag{B6}$$

where we have converted the sum back to an integral in the second line. It is possible to prove using this expression that $\sigma(b_v) \geq 1/\mathrm{SNR}$, so our "refined" estimate for $\sigma(b_v)$ is more pessimistic than the back-of-the-envelope estimate $\sigma(b_v) \approx 1/\mathrm{SNR}$, as anticipated. In this work, wherever a prior on b_v is assumed, the refined estimate derived here is used.

[1] R. A. Sunyaev and I. B. Zeldovich, Mon. Not. R. Astron. Soc. **190**, 413 (1980).
[2] N. Aghanim, K. M. Górski, and J.-L. Puget, Astron. Astrophys. **374**, 1 (2001).
[3] S. Bhattacharya and A. Kosowsky, Astrophys. J. Lett. **659**, L83 (2007).
[4] P. G. Ferreira, R. Juszkiewicz, H. A. Feldman, M. Davis, and A. H. Jaffe, Astrophys. J. Lett. **515**, L1 (1999).
[5] C. Hernández-Monteagudo, L. Verde, R. Jimenez, and D. N. Spergel, Astrophys. J. **643**, 598 (2006).
[6] P. Ade *et al.*, J. Cosmol. Astropart. Phys. 02 (2019) 056.
[7] K. M. Smith, M. S. Madhavacheril, M. Münchmeyer, S. Ferraro, U. Giri, and M. C. Johnson, arXiv:1810.13423.
[8] M. Münchmeyer, M. S. Madhavacheril, S. Ferraro, M. C. Johnson, and K. M. Smith, Phys. Rev. D **100**, 083508 (2019).
[9] D. Alonso, T. Louis, P. Bull, and P. G. Ferreira, 2016.
[10] S. Bhattacharya and A. Kosowsky, Phys. Rev. D **77**, 083004 (2008).

[11] S. DeDeo, D. N. Spergel, and H. Trac, arXiv:astro-ph/0511060.
[12] R. Keisler and F. Schmidt, Astrophys. J. Lett. **765**, L32 (2013).
[13] E.-M. Mueller, F. de Bernardis, R. Bean, and M. D. Niemack, Astrophys. J. **808**, 47 (2015).
[14] E.-M. Mueller, F. de Bernardis, R. Bean, and M. D. Niemack, Phys. Rev. D **92**, 063501 (2015).
[15] N. Battaglia, J. Cosmol. Astropart. Phys. 08 (2016) 058.
[16] S. Flender, D. Nagai, and M. McDonald, Astrophys. J. **837**, 124 (2017).
[17] P. C. Boyle (Chime/Frb Collaboration), Astronomer's Telegram 11901 (2018), http://www.astronomerstelegram.org/?read=11901.
[18] P. Chawla *et al.*, Astrophys. J. **844**, 140 (2017).
[19] R. M. Shannon *et al.*, Nature (London) **562**, 386 (2018).
[20] L. B. Newburgh *et al.*, Ground-based and Airborne Telescopes VI, in *Proceedings of SPIE* (2016), Vol. 9906, p. 99065X.
[21] S. P. Tendulkar *et al.*, Astrophys. J. Lett. **834**, L7 (2017).
[22] K. Dolag, B. M. Gaensler, A. M. Beck, and M. C. Beck, Mon. Not. R. Astron. Soc. **451**, 4277 (2015).
[23] M. McQuinn, Astrophys. J. Lett. **780**, L33 (2014).
[24] V. Ravi, Astrophys. J. **872**, 88 (2019).
[25] A. Fialkov and A. Loeb, J. Cosmol. Astropart. Phys. 05 (2016) 004.
[26] K. W. Masui and K. Sigurdson, Phys. Rev. Lett. **115** (2015).
[27] M. Jaroszynski, Mon. Not. R. Astron. Soc. **484**, 1637 (2019).
[28] DESI Collaboration *et al.*, arXiv:1611.00036.
[29] K. Ioka, Astrophys. J. Lett. **598**, L79 (2003).
[30] S. Chatterjee *et al.*, Nature (London) **541**, 58 (2017).
[31] J. M. Cordes and T. J. W. Lazio, arXiv:astro-ph/0207156.
[32] K. N. Abazajian *et al.*, arXiv:1610.02743.
[33] A.-S. Deutsch, E. Dimastrogiovanni, M. C. Johnson, M. Münchmeyer, and A. Terrana, Phys. Rev. D **98**, 123501 (2018).
[34] M. Münchmeyer, M. S. Madhavacheril, S. Ferraro, M. C. Johnson, and K. M. Smith, Phys. Rev. D **100**, 083508 (2019).
[35] N. Kaiser, Mon. Not. R. Astron. Soc. **227**, 1 (1987).
[36] N. S. Sugiyama, T. Okumura, and D. N. Spergel, J. Cosmol. Astropart. Phys. 01(2017) 057.
[37] C. M. Hirata, Mon. Not. R. Astron. Soc. **399**, 1074 (2009).
[38] B. Stappers and M. Kramer, in *Proceedings of MeerKAT Science: On the Pathway to the SKA, Stellenbosch, South Africa (MeerKAT2016)* (2016), p. 9.
[39] J. P. Macquart *et al.*, *Advancing Astrophysics with the Square Kilometre Array (AASKA14)* (2015), p. 55.
[40] Y. Fujita, T. Akahori, K. Umetsu, C. L. Sarazin, and K.-W. Wong, Astrophys. J. **834**, 13 (2017).
[41] J. B. Muñoz and A. Loeb, Phys. Rev. D **98**, 103518 (2018).
[42] M. P. van Daalen, J. Schaye, C. M. Booth, and C. Dalla Vecchia, Mon. Not. R. Astron. Soc. **415**, 3649 (2011).
[43] T. Eifler, E. Krause, S. Dodelson, A. R. Zentner, A. P. Hearin, and N. Y. Gnedin, Mon. Not. R. Astron. Soc. **454**, 2451 (2015).
[44] A. Schneider, R. Teyssier, J. Stadel, N. E. Chisari, A. M. C. Le Brun, A. Amara, and A. Refregier, J. Cosmol. Astropart. Phys. 03 (2019) 020.
[45] E. Semboloni, H. Hoekstra, J. Schaye, M. P. van Daalen, and I. G. McCarthy, Mon. Not. R. Astron. Soc. **417**, 2020 (2011).